

300
7/8/81
M.E.

②

Bins-196
NTIS-25

1h. 2808

DOE/ET/10623-T1

IMPROVED TECHNIQUES FOR GASIFYING COAL

Twelfth Quarterly Report for Period April 1-June 30, 1979

By
Robert A. Graff
Alberto I. LaCava

MASTER

Work Performed Under Contract No. AS01-76ET10623

The City College of The
City University of New York
New York, New York

**F
O
S
S
I
L
E
S
H
I
P
R
E
P
A
R
E
D
B
Y**



U. S. DEPARTMENT OF ENERGY

DISCLAIMER

This report was prepared as an account of work sponsored by an agency of the United States Government. Neither the United States Government nor any agency Thereof, nor any of their employees, makes any warranty, express or implied, or assumes any legal liability or responsibility for the accuracy, completeness, or usefulness of any information, apparatus, product, or process disclosed, or represents that its use would not infringe privately owned rights. Reference herein to any specific commercial product, process, or service by trade name, trademark, manufacturer, or otherwise does not necessarily constitute or imply its endorsement, recommendation, or favoring by the United States Government or any agency thereof. The views and opinions of authors expressed herein do not necessarily state or reflect those of the United States Government or any agency thereof.

DISCLAIMER

Portions of this document may be illegible in electronic image products. Images are produced from the best available original document.

DISCLAIMER

"This book was prepared as an account of work sponsored by an agency of the United States Government. Neither the United States Government nor any agency thereof, nor any of their employees, makes any warranty, express or implied, or assumes any legal liability or responsibility for the accuracy, completeness, or usefulness of any information, apparatus, product, or process disclosed, or represents that its use would not infringe privately owned rights. Reference herein to any specific commercial product, process, or service by trade name, trademark, manufacturer, or otherwise, does not necessarily constitute or imply its endorsement, recommendation, or favoring by the United States Government or any agency thereof. The views and opinions of authors expressed herein do not necessarily state or reflect those of the United States Government or any agency thereof."

This report has been reproduced directly from the best available copy.

Available from the National Technical Information Service, U. S. Department of Commerce, Springfield, Virginia 22161.

Price: Printed Copy A03
Microfiche A01

NOTICE
PORTIONS OF THIS REPORT ARE ILLEGIBLE.

It has been reproduced from the best available copy to permit the broadest possible availability.

DOE/ET/10623--T1

DE81 018175

IMPROVED TECHNIQUES FOR GASIFYING COAL

Twelfth Quarterly Report
April 1, 1979 - June 30, 1979

Robert A. Graff
Alberto I. LaCava

The City College of The
City University of New York
New York, New York 10031

Prepared for the United States
Department of Energy

Under Contract No. EX-76-S-01-2340

ACKNOWLEDGMENTS

Substantial contributions to this report were made by:

Amos A. Avidan, Graduate Research Assistant

William Chen, Graduate Research Assistant

John O'Mara, Graduate Research Assistant

Shi-Jin Shen, Graduate Research Assistant

Dr. Joseph Yerushalmi has joined the Electric Power Research Institute, Palo Alto, CA. He has, however, continued to review and advise on the work reported here.

TABLE OF CONTENTS

| | |
|---|----|
| SUMMARY OF PROGRESS..... | 1 |
| I. High Velocity Fluidized Beds..... | 1 |
| II. Flash Hydrogenation..... | 1 |
| III. Flash Hydrolysis..... | 2 |
| DETAILED DESCRIPTION OF TECHNICAL PROGRESS..... | 3 |
| I. STUDIES OF HIGH VELOCITY FLUIDIZED BEDS..... | 3 |
| I.1 Work Accomplished: Bed Expansion of Fine Powders and the Phenomenon of Clustering..... | 3 |
| I.1.1 INTRODUCTION..... | 3 |
| I.1.1.a The Effect of Particle Size Distribution on Bed Expansion of Fine Powders..... | 5 |
| I.1.1.b Bed Expansion of Fine Powders in the Dense Conveying Regime..... | 6 |
| I.1.2 THE INDEX N IN THE MODIFIED RICHARDSON-ZAKI APPROACH..... | 6 |
| I.1.3 U^*_T IN THE MODIFIED RICHARDSON-ZAKI APPROACH..... | 17 |
| I.1.4 REFERENCES..... | 25 |
| I.2 WORK FORECAST FOR THE NEXT QUARTER..... | 27 |
| II. FLASH HYDROGENATION..... | 28 |
| II.1 Work Accomplished..... | 28 |
| II.1.1 Yield Correlations..... | 28 |
| II.1.2 Discussion..... | 37 |
| II.1.3 Liquids Characterization..... | 39 |
| II.2 WORK FORECAST FOR THE NEXT QUARTER..... | 42 |
| III. FLASH HYDROLYSIS..... | 43 |
| III.1 Work Accomplished..... | 43 |
| III.2 WORK FORECAST FOR THE NEXT QUARTER..... | 43 |
| CONCLUSIONS..... | 45 |
| I. High Velocity Fluidized Beds..... | 45 |
| II. Flash Hydrogenation..... | 46 |
| III. Flash Hydrolysis..... | 46 |

SUMMARY OF PROGRESS

I. HIGH VELOCITY FLUIDIZED BEDS

Bed expansion of three fine group A powders is described by a modified Richardson and Zaki correlation. The two parameters in this correlation are shown to be inherently tied to the clustering behavior of fine powders. Particle properties affect bed expansion, but the main parameter is shown to be particle size distribution. The index n in the modified Richardson-Zaki correlation is thought of as a measure of segregation of the bed; being high (~ 10) in the slugging regime and low (~ 5) in the more homogeneous turbulent regime. Cluster size and voidage are calculated from the two parameters in the Richardson-Zaki approach and some light is thrown in the phenomenon of clustering. This aggregation of fine powders is thought to be a dynamic phenomenon, with particles quickly moving in and out of clusters. Thus the hydrodynamics of the bed can be described as somewhere between a hard sphere picture of clusters and that of a bed composed of individual particles. To be able to predict bed expansion, these cluster properties prove useful. However, because of the dual nature of these clusters, it is believed that the effectiveness of the bed as, for example, a catalytic reactor, will not be impaired.

II. FLASH HYDROGENATION

Empirical yield correlations involving two coal properties as independent parameters were developed using the technique of stepwise regression to identify the parameter pairs that provide the best fit. These correlations of yields of the individual products are valid for the reaction conditions employed. Modelling considerations offer a theoretical basis for the correlations presented.

The gravimetric determination of the SESC fraction is affected by errors due to the presence of silica gel from the column. Pre-washing with solvents did not eliminate the problem. A high pressure GPC column is now being used that reduces analysis time compared with the low-pressure column previously used. A comparison of coal-derived liquids by GPC shows the power of this technique.

III. FLASH HYDROLYSIS

A modification of the electrical system of the flash hydrolysis reactor has been made which will allow heating rate to be adjusted at will. This is in preparation for a study of the effect of heating rate on hydrolysis yield to be made in the next quarter.

DETAILED DESCRIPTION OF TECHNICAL PROGRESS

I. STUDIES OF HIGH VELOCITY FLUIDIZED BEDS

I.1 WORK ACCOMPLISHED: Bed Expansion of Fine Powders and the Phenomenon of Clustering.

I.1.1 INTRODUCTION

Bed expansion of FCC in all fluidization regimes was described by the modified Richardson-Zaki approach in the 11th Quarterly report. The correlation takes the form:

$$U_g/U_T^* = \epsilon^n \quad (1)$$

where U_g is the superficial gas velocity, ϵ is the average voidage in the central part of the bed, U_T^* is the modified terminal velocity (or the equivalent cluster terminal velocity $U_T^* \gg U_t$, the single particle terminal velocity).

Experiments were also conducted in the circulating and expanded top systems for the other two group A powders, HFZ-20 and Dicalite 4200. The results for the fast fluidization region suffer from too much scatter for these two powders and so only a comparison to FCC in the slugging, turbulent, and dense conveying regime will be attempted. A comparison for the slugging and turbulent regimes for the three powders (all "used") is shown in Table I-1.

There seems to be a good deal of similarity between FCC and HFZ-20. Their n values are very close in both the slugging and turbulent regimes, and their U_T^*/U_T values seem to be linearly proportional to their respective $\rho_s dp$ (or G_a) values. This indicates that powders similar in size distribution behave similarly in the slugging and turbulent regimes, their n values are ~9 (slugging) and ~4.7 (turbulent). Their U_T^* values are proportional to particle properties, as shown for HFZ-20 and FCC.

Dicalite, on the other hand, exhibits a markedly different behavior, both visually and as indicated in Table I-1. The much

Table I-1. Expansion Properties of Three Group A Powders ("Used") in the Slugging and Turbulent Regimes.

| Powder | $\rho_s dp$ (g/cm ² $\times 10^3$) | G_a^* $\times 10^{-8}$ | Slugging Regime | | | Transition to Turbulence Velocity (m/s) | Turbulent Regime | | | Transition to Fast Fluidization (m/s) |
|----------|--|-----------------------------|-----------------|---------------|---------------------|---|------------------|---------------|---------------------|---------------------------------------|
| | | | n | U_T^* (m/s) | $\frac{U_T^*}{U_T}$ | | n | U_T^* (m/s) | $\frac{U_T^*}{U_T}$ | |
| FCC | 5.24 | 1.84 | 9.2 | 22.5 | 290 | 0.37 | 5 | 3.4 | 43.7 | 1.4 |
| HFZ-20 | 7.11 | 2.49 | 8.3 | 38.7 | 365 | 0.88 | 4.4 | 6.3 | 59.4 | 1.8-2.1 |
| Dicalite | 5.51 | 1.88 | 46 | 853 | 3.8×10^4 | 0.52 | 14 | 5.0 | 220 | 1.1 |

$$*G_a = \frac{\rho_g (\rho_s - \rho_g) g d^3}{\mu^2}$$

(2)

higher values of U_T^* and n for Dicalite at the lower gas velocities (slugging and turbulent regimes) are attributed to its cohesiveness, especially when in a humid atmosphere. Dicalite is on the border between Group A and C of Geldart's classification and in these two regimes its cohesive properties predominate.

I.1.1.a: The Effect of Particle Size Distribution on Bed Expansion of Fine Powders

The size distribution of the particles has a large effect on U_T^* and a small effect on n . This was shown in our expanded top bed when one compares "fresh" catalyst (with a large fines fraction) to "used" catalyst that has been run in the recirculating system for several hours and thus lost one half of the smaller particles. All our reported results, so far, save for the comparison in Table I-2, are for "used" catalyst.

Table I-1. Comparison between "Fresh" and "Used" Catalyst

| Powder | Slugging Regime | | Turbulent Regime | |
|---------------|-----------------|------|------------------|-----|
| | U_T^* (m/s) | n | U_T^* (m/s) | n |
| FCC ("Fresh") | 12.2 | 10.2 | 2.8 | 6 |
| FCC ("Used") | 22.6 | 9.2 | 3.4 | 5 |
| HFZ ("Fresh") | 30.5 | 10 | 4.5 | 5.1 |
| HFZ ("Used") | 38.7 | 8.3 | 6.3 | 4.4 |

Little effect on n is shown for both FCC and HFZ. However a considerable difference in U_T^* is noted: "fresh" catalyst has a lower value than used catalyst indicating better fluidization of a powder that contains a larger fines fraction. The "used" powder has less fines, thus clusters to a larger degree than the "smooth" fresh catalyst, causing a large effective U_T^* .

I.1.1.b: Bed Expansion of Fine Powders in the Dense Conveying Regime ($\epsilon > 0.95$)

All three powders behave similarly in the dense conveying regime. This is shown in Figure I-1. Figure I-1 shows the variation in the index n , with the solid rate in the dense conveying regime. Despite some scatter, there seems to be no statistically significant difference between the three powders, which is surprising in the case of Dicalite. Figure I-1.b, giving U_T^* vs. G_s , shows an even better correlation.

If one considers U_T^* to be a measure of cluster size and density (an "effective" terminal velocity), it seems that all three powders give rise to similar clusters for $\epsilon > 0.95$. Figure I-1.c shows the transition velocity from fast fluidization to dense conveying (i.e., the gas velocity at $\epsilon = 0.945$) vs. solid rate, and again, all three powders behave similarly.

I.1.2 The Index n in the Modified Richardson-Zaki Approach

The index n should assume the value of 4.65 for fine powders. Indeed, for FCC and HFZ, as well as for the cracking catalysts used by Canotenuto (1974) and Massimilla (1971), $n \approx 5$ in the turbulent regime. This view of the turbulent regime is supported by visual observations in our transparent equipment. The transition to turbulence is associated with the break-up of the slugs. On the whole the voids are smaller, and moreover, they appear and disappear in contrast to the slugging regime where usually one can follow a single slug from the bottom of the bed to the top.

Thus the index n can be viewed as a measure of the homogeneity of the fluidized bed. For fine cracking catalysts it seems to be only slightly dependent on particle properties or size distribution, which strongly affect U_T^* . In the slugging regime, our data as well as the above-mentioned data from the literature yield values of the index n which average around 10, or twice its value in the turbulent

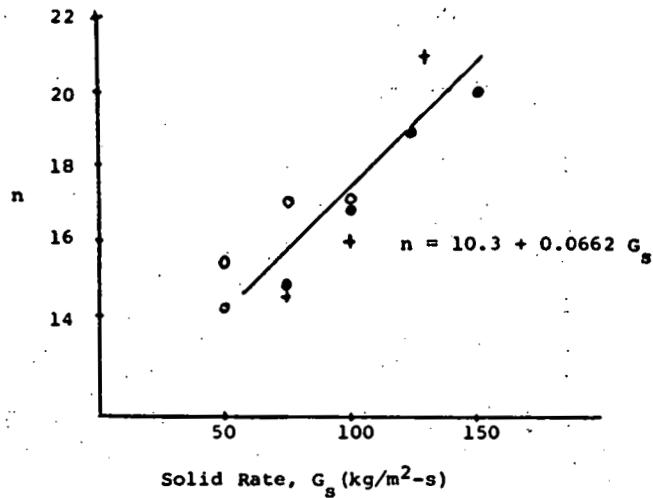


Fig. I-la. The index n in the dense conveying regime for three Group A powders.

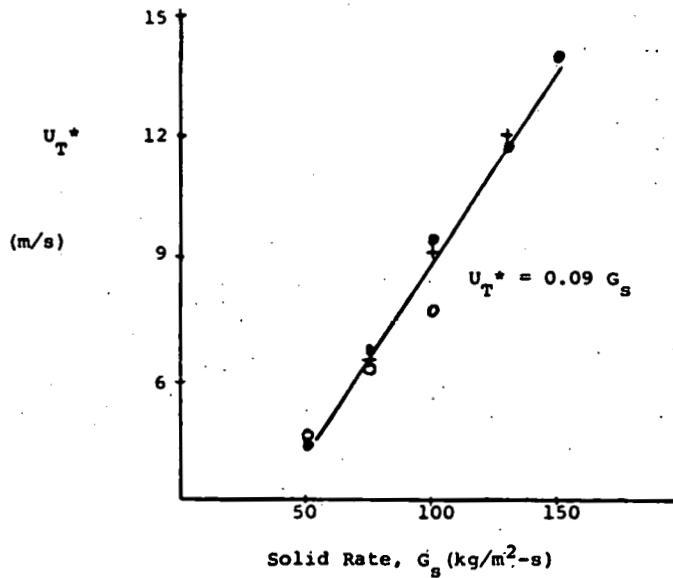


Fig. I-lb. U_T^* in the dense conveying regime for three Group A powders.

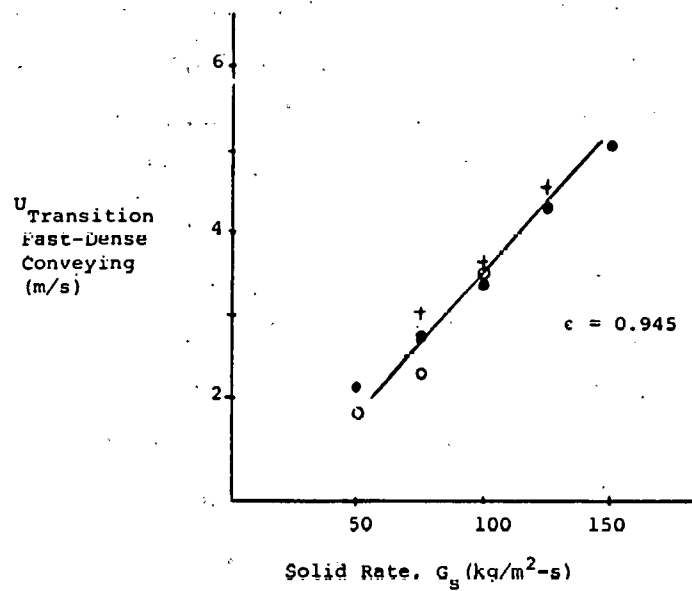


Fig. I-1c. Transition velocity from fast fluidization to dense conveying for three Group A powders.

Symbols used in Fig. 3.9

- † - HFZ-20
- - Dicalite
- - FCC

regime. Mogan, Taylor and Booth (1970/71) summarize data from several investigators showing n values from 4 - 10 for fine solids. Analysis of the Data of Zenz and Othmer (1960) shows a change in slope, or in the index n , when a transition from bubbling to slugging occurs. Thus, the range 4 - 10 reported by Mogan et al, can be viewed as representing data from the two regimes, the lower values in the bubbling regime, and the higher n values in the slugging regime. This reinforces the notion that the index n is a degree of segregation showing the greatest degree of inhomogeneity for the slugging regime.

Capes (1974) has suggested that high values of n reported by Mogan, et al. may be due to increased particle volume caused by agglomeration or irregular particle shape. This can be tied to our representation of segregation in the slugging regime, since the formation of slugs is probably enhanced by the agglomerative nature of the particles. Capes presents an approach that takes this agglomeration into account, and by making use of an "effective" porosity represents bed expansion by:

$$\frac{U}{U_T^*} = (1-KC)^n \quad (3)$$

where: $(1-KC) = \epsilon_e$ effective porosity (4)

$(1-C) = \epsilon_a$ apparent porosity (5)

Values of $K > 1$ indicate clustering and indeed this causes the effective porosity to be less than the apparent one. It is interesting to compare this approach to Yerushalmi et al. (1978), shown in Equation 6:

$$(1 - \epsilon_a) = (1 - \epsilon_e) (1 - \epsilon_c) \quad (6)$$

where ϵ_c , the cluster voidage, is not assumed to be ϵ_{mf} for the moment. Substituting Equations 4 and 5 into Equation 6 one gets:

$$K = \frac{1}{1 - \epsilon_c} \quad \text{or} \quad (7)$$

$$\epsilon_c = 1 - \frac{1}{K} \quad (8)$$

Let us examine the K values reported by Capes:

Table I-2: Cluster Voidage from K Values Reported by Capes (1974)

| K | ϵ_c |
|-----|--------------|
| 0.8 | -0.25 |
| 1 | 0 |
| 1.2 | 0.17 |
| 1.4 | 0.29 |
| 1.7 | 0.41 |

In this analysis it is hard to attach physical sense to $K < 1$, which gives negative values to ϵ_c . For spherical particles values of $K < 1.3$ should be used, and if one assumes minimum fluidization voidage for the clusters, one should use $K > 1.7$, which is the highest value reported by Capes. It is clear that the "clusters" reported by Capes and the same concept as used by us are different. While Capes reports cluster size of 100-260 μm , which is in the range of the largest particles used by Mogan et al., much larger clusters are evident in our work.

The results of Mogan, Taylor and Booth (1969), are important because of the limited high pressure data available, but a 1.75 cm ID tube was used. They observed a "predominantly downward motion at the tube wall," which raises questions as to the magnitude of wall effects. The dependence of bed expansion on bed diameter was shown to be quite strong. In general, the voidage will decrease strongly in going from $D_t = 1.75$ cm to D_t say, of 15 cm. This would offer an alternative explanation to the high value of n as being a small diameter phenomenon in this case.

Our approach, on the other hand, is to view the index n as a degree of segregation in a slugging bed of fine solids caused largely by particle agglomeration. Thus, large values of the index n arise naturally and need not be corrected. These values of n can be obtained from the Richardson-Zaki equation if one uses D_c , or an "equivalent" cluster diameter, instead of d_p , the single particle diameter.

For FCC and HFZ the appropriate equation is:

$$n = \left(4.35 + 17.5 \frac{D_c}{Dt}\right) Re_t^{-0.03} \quad (9)$$

Note that the single particle Reynolds number is used in choosing the appropriate Reynolds number range and in Equation 9, while D_c is used for dp . The rationale for this choice is that clustering is a dynamic phenomenon, particles move in and out of clusters - a phenomenon that is supported by high velocity movies taken at CCNY and by DeLasa and Gau (1973). Thus, the single particle properties, as well as its Reynolds number, are still important. Clustering is taken into account as a segregation causing phenomenon, which is relative to D_t , the tube diameter. Obviously, Equation 9 is only a first approximation, but some order of magnitude values of D_c can be obtained from it (and experimental values of n) and compared to the cluster diameter calculated by Yerushalmi et al. (1978).

Table I-3 Cluster Diameters for FCC

| Regime | D_c from Eq. 9 (cm) | D_c from Yerushalmi et al. (cm) |
|-----------|-----------------------|-----------------------------------|
| Slugging | 3.9 | ~ 3.0 |
| Turbulent | 0.4 | 0.7-1.5 |

An order of magnitude agreement and the same trend are shown for the cluster diameter calculated by both methods in Table I-3. The same trend continues into the fast fluidization regime, n values are getting smaller, and so is D_c as calculated by Yerushalmi et al. While this can be viewed as encouraging, one should not forget that we refer to clusters as a concept rather than as hard spheres of a diameter D_c . As was pointed out before, clustering is

a complex dynamic phenomenon. One should keep in mind the following important features of clusters:

a) A size distribution rather than a single diameter is more likely to represent cluster size.

b) The cluster voidage, ϵ_i , as well as the cluster size affects the "effective terminal velocity." This voidage can vary with cluster size, time, and gas and solid fluxes. The effect of this cluster voidage on the slip velocity is elaborated upon in the next subsection.

c) Clustering is a dynamic phenomenon, particles move into clusters, are stripped off by the rising gas; smaller clusters coalesce to large ones, which in turn break up. DeLasa and Gau (1973) found that this observed clustering does not affect conversion in a catalytic reaction. This would seem to indicate that clustering is not a segregative phenomenon as far as gas-solid contact is concerned. It would seem plausible to assume that either or both of the following is taking place: more gas than previously assumed is travelling through the cluster phase (causing larger cluster voidages than minimum fluidization; the characteristic time distribution associated with a particle being in a cluster is small when compared to the average gas residence time.

d) Our visual observations and high velocity movies support the dynamic picture presented above. It also seems that most rising clusters are elongated in shape, explaining the observed drag reduction by the shielding effect of long chains of spheres. This has been discussed by Avidan (1979).

All of these factors help illustrate the complexity of the clustering phenomenon. It is clear that a simple "hard sphere" picture is inadequate when describing clustering. A more quantitative comparison between the "hard sphere" model and the actual slip velocity is presented in the following subsection.

In the fast fluidization and dense conveying regimes both n and U_T^* become dependent on solid rate. The dependence of the index n on solid rate was shown to be linear for all three group A powders (Figure I-1.a) investigated in the dense conveying regime, and can be described by:

$$\begin{array}{l} \text{dense} \\ \text{conveying} \\ \text{fine powders} \end{array} \quad n = 10.3 + 0.0662G_s \quad (10)$$

The same linear dependence is shown for FCC in the fast fluidization regime (Figure I-2):

$$\begin{array}{l} \text{FCC} \\ \text{fast fluidization} \end{array} \quad n = 0.0482G_s \quad (11)$$

Both regimes show an increase in the value of n , or the degree of segregation, with increasing the solid rate.

A different approach towards understanding the significance of the exponent n allows us to get a handle on cluster voidage. In this approach the clusters are considered more "tightly packed," so that their cluster size and voidage would cause an effective behavior similar to large particle fluidization, i.e., n values from Equation 9 would be in the 2.4-3 range. An effective, rather than the apparent voidage should then be used to represent bed expansion (in the form of Equation 1). Both voidages are represented in Figure I-3, which is similar to the curves presented by Capes (1974).

Thus, this approach would consider n values to be those of large particles, of the same diameter as D_c . The connection between the apparent and effective voidages is through the cluster voidage, Equation 9. The cluster diameter is calculated from:

$$\epsilon_c = 1 - \frac{1 - \epsilon_a}{1 - \epsilon_a^{n/n'}} \quad (12)$$

If $n' = 2.4$ would have been used throughout all fluidization regimes, the cluster voidage of Table I-4 are calculated.

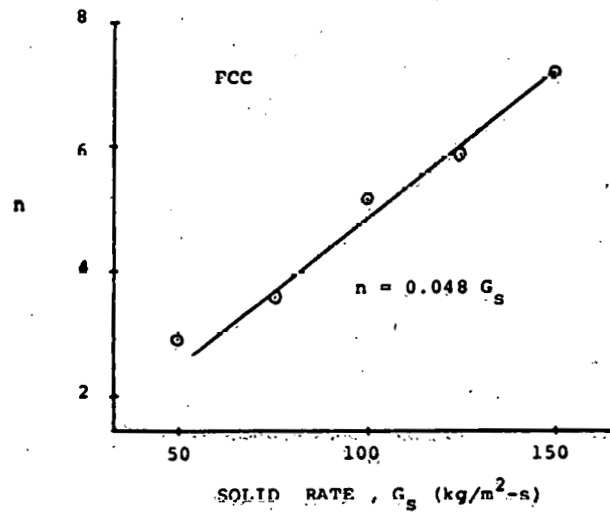
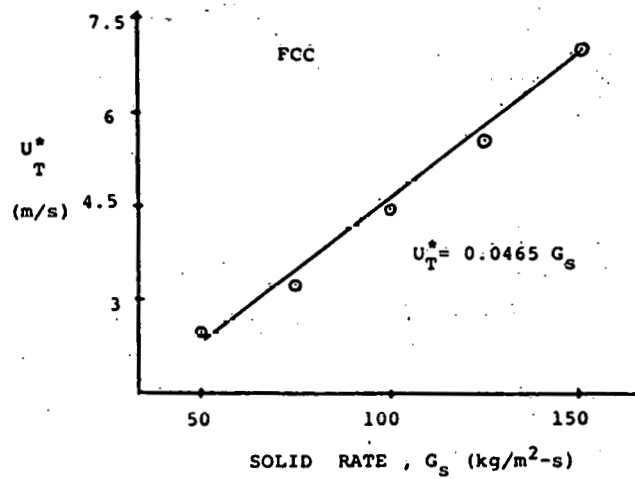


Fig. I-2. The index n and U_T^* for FCC ("used") in the fast fluidization regime.

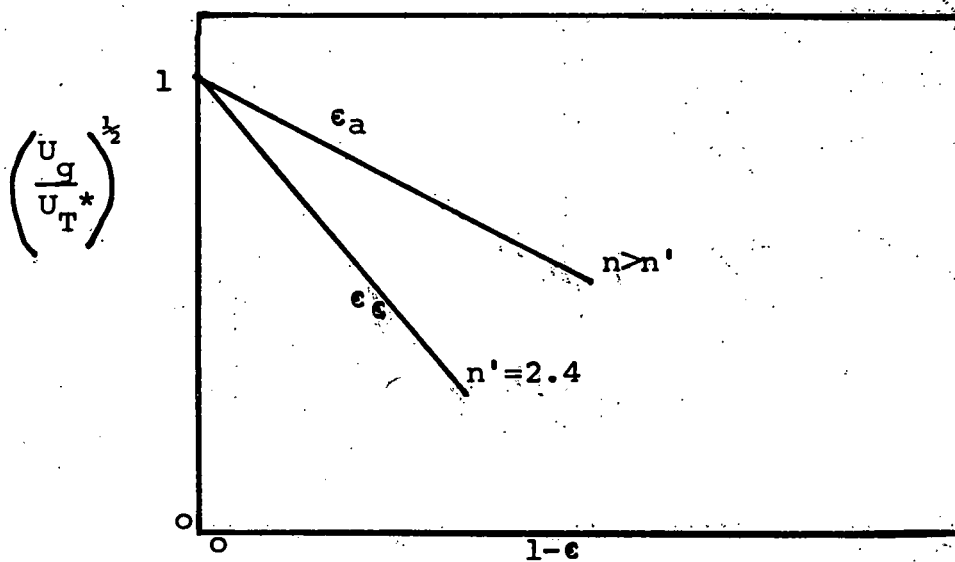


Fig. I-3. Schematic representation of bed expansion in one fluidization regime.

Table I-4 - Cluster Voidage Calculated from Equation (12)

| Regime | n | Apparent Voidage ϵ_a | Cluster Voidage ϵ_c | Effective Voidage ϵ_e |
|-----------|-----|-------------------------------|------------------------------|--------------------------------|
| Slugging | 9.2 | 0.54 | 0.49 | 0.09 |
| | | 0.6 | 0.53 | 0.14 |
| Turbulent | 5 | 0.64 | 0.41 | 0.39 |
| | | 0.7 | 0.43 | 0.48 |
| | | 0.75 | 0.45 | 0.55 |

Fast Fluidization

| $G_s = 50 \text{ kg/m}^2\text{-s}$ | | | $G_s = 100 \text{ kg/m}^2\text{-s}$ | | | $G_s = 150 \text{ kg/m}^2\text{-s}$ | | |
|------------------------------------|--------------|--------------|-------------------------------------|--------------|--------------|-------------------------------------|--------------|--------------|
| n = 2.9 | | | n = 9.5 | | | n = 7.2 | | |
| ϵ_a | ϵ_c | ϵ_e | ϵ_a | ϵ_c | ϵ_e | ϵ_a | ϵ_c | ϵ_e |
| 0.82 | 0.16 | 0.79 | 0.84 | 0.43 | 0.72 | 0.86 | 0.62 | 0.64 |
| 0.87 | 0.16 | 0.85 | 0.90 | 0.44 | 0.82 | 0.90 | 0.63 | 0.73 |
| 0.95 | 0.17 | 0.94 | 0.95 | 0.45 | 0.91 | 0.95 | 0.65 | 0.86 |
| Dense Conveying n = 14.2 | | | n = 9.4 | | | n = 20 | | |
| ϵ_a | ϵ_c | ϵ_e | ϵ_a | ϵ_c | ϵ_e | ϵ_a | ϵ_c | ϵ_e |
| 0.97 | 0.82 | 0.84 | 0.97 | 0.73 | 0.89 | 0.97 | 0.87 | 0.78 |

The following features are presented by Table I-4:

a) The values of the effective voidage are very low in the slugging regime. It can be concluded that this method is not suitable for the slugging regime where the index n represents gross segregation into the slug and dense phases rather than clustering.

b) For the more homogeneous higher velocity regimes reasonable values for the cluster voidage are obtained. It should be noted that the cluster voidage remains relatively constant in each fluidization regime, increasing slightly as the gas velocity is raised.

c) In the turbulent regime, the cluster voidage is close to minimum fluidization voidage, an assumption which is often made.

d) In the fast and dense conveying regimes the cluster voidage is a function of the solid rate, being very low for $G_s = 50$ $\text{kg/m}^2\text{-s}$.

For this low solid rate it is hard to attach physical significance to $\epsilon_c = 0.16$ unless one can assume very small clusters, or an almost uniform suspension. The higher solid rates present reasonable cluster voidages, from minimum fluidization voidage ($G_s = 100$ $\text{kg/m}^2\text{-s}$) to $\epsilon_c = 0.63$ for $G_s = 150$ $\text{kg/m}^2\text{-s}$. The higher slip velocity associated with the higher solid rate is causing a higher cluster voidage. All three voidages, ϵ_a , ϵ_c , and ϵ_o approach one when the dilute transport regime is approached.

I.1.3 U_T^* in the Modified Richardson-Zaki Approach

The value of U_T^* is thought to represent the size and density of clustering in the suspension. It has a high value, many times the single particle terminal velocity, in the slugging regime and it decreases considerably on transition to turbulence takes place. For both HFZ-20 and FCC ("used) U_T^*/U_T values in the turbulent and

slugging regime are linearly dependent on their respective $\rho_s d_p$ products, or Galileo numbers. This relationship shown in Table I-1 cannot be taken to include our "fresh" catalysts, Dicalite, or the fine solids used by other investigators. The culprit seems to be the effect of the size distribution shown in Table I-2. "Fresh" catalysts show markedly lower values of U_T^* in both the slugging and turbulent regimes than "used" catalysts. Thus, unless the effect of the size distribution, which seems stronger than particle properties, can be taken into account, no general dependence on $\rho_s d_p$ can be suggested. The strong dependence of bed expansion on size distribution was shown by Rowe et al. (1978) and qualitatively their results show the same trend: the higher the fines fraction the higher the voidage at the same gas velocity. Since the index n does not vary much, this causes a much lower value for U_T^* . A reduction in the effective cluster size seems to take place when more gas flows in the dense phase.

Much like the index n , U_T^* seems to decrease in going to the turbulent regime, suggesting more homogeneity. U_T^* increases with increasing solid rate in both the fast and dense conveying regimes, qualitatively agreeing with the picture of increased clustering as the solid rate increases. It is not clear how an "equivalent" cluster diameter can be calculated from U_T^* . As an exercise, a simple approach is illustrated in Table I-5 where a cluster diameter is calculated by using:

$$U_T^* = \left(\frac{3.1g(\rho_c - \rho_g)D_c}{\rho_g} \right)^{1/2} \quad (13)$$

for

$$Re_c = \frac{D_c \rho_g U_T^*}{\mu} > 500 \quad (\text{Kunii and Levenspiel, 1969})$$

Table I-5: Cluster Diameter Calculated from U_T^* for "Used" FCC

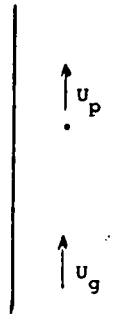
| Regime | U_T^* (m/s) | D_c (cm) |
|---|------------------|---------------|
| Slugging | 22.6 | 1.92 |
| Turbulent | 3.4 | 0.0435 |
| Fast $G_s = 50 \frac{\text{kg}}{\text{m}^2\text{-s}}$ | 2.5 | 0.0235 |
| 75 | 3.3 | 0.0410 |
| 100 | 4.5 | 0.0763 |
| 125 | 5.6 | 0.118 |
| 150 | 7.2 | 0.195 |
| Dense Conveying $G_s = 50 \text{ kg/m}^2\text{-s}$ | 4.6 | 0.080 |
| 75 | 6.4 | 0.154 |
| 100 | 9.4 | 0.333 |
| 125 | 11.6 | 0.507 |
| 150 | 13.7 | 0.707 |

The qualitative agreement with D_c values, calculated from the index n , is shown for the slugging and turbulent regimes in Tables I-3 and I-4. The variation of U_T^* with solid rate in the fast fluidization regime for FCC is shown in Figure I.3.b where it is shown that $U_T^* = 0.0465 G_s$. In the dense conveying regime, all three powders investigated seem to follow the same linear relationship $U_T^* = 0.09 G_s$, possibly suggesting that all three cluster to the same degree in that regime. This relationship is shown in Figure I-1.b.

It is interesting to look at the connection between the effective terminal velocity and the slip velocity. When one starts with a single particle conveyed by a gas with a superficial velocity, U_g , the slip velocity is equal to the single particle terminal velocity. This is illustrated in Figure I-4.a. Upon adding more particles, but keeping the suspension dilute one can observe uniformly dispersed particles - especially when wall effects are negligible. For this situation, depicted in Figure I-4b, the slip velocity is less than the single particle terminal velocity, and the phenomenon is known as hindered settling. While no data are presented here for pneumatic conveying, visual observations lead us to believe that particles are not truly uniformly dispersed and one can always detect some clustering and recirculating especially in the vicinity of the walls. This deviation from a uniformly dispersed suspension is more pronounced at higher solid rates, or lower gas velocities. At a voidage of approximately 0.98 or lower, the uniform suspension structure breaks down and the agglomerative nature of the suspension is evident. Particles rise in center, in the form of twisting chains, of varying lengths and widths. These chains or strands are broken and reformed and some are falling back, especially in the vicinity of the walls. Some agglomerations of

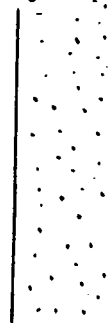
a) A single particle

$$U_{slip} = U_g - U_p = U_T$$



b) Uniformly dispersed dilute suspension

$$\frac{U_g}{\epsilon} - U_p = \epsilon^n U_T$$



$U_{slip} < U_T$
"hindered settling"

c) "dense conveying"

$$U_{slip} > U_T$$

$$\frac{U_g}{\epsilon} - U_p < \epsilon^n U_T^*$$



clustering
and
recirculation

d) Fast fluidization

$$\frac{U_g}{\epsilon} - U_p \leq \epsilon^n U_T^*$$

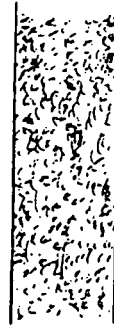


Fig. I-4. Slip Velocity in various fluidization regimes.

particles seem to be almost stagnant at the wall, they creep down (or up at higher gas velocities) and are constantly stripped of particles and then replaced by new clusters, seemingly thrown off the center region of the tube. This picture is typical of the proposed dense conveying regime, and is represented schematically in Figure I-4.c.

Both clustering and solid recirculation are causing a reversal in the magnitude of the slip velocity, and one obtains slip velocities much higher than the single particle terminal velocity. The suspension "effective terminal velocity" U_T^* was calculated, along with the index n , from the expansion data. It is evident that all values of U_T^* , in the dense conveying regime, are more than an order of magnitude greater than the single particle terminal velocity. These values of U_T^* lead to cluster sizes in the range of 0.08-0.707 cm as opposed to a particle mean diameter of 0.0049 cm. If one can consider these clusters as rigid spheres one would expect a modified equation for the slip velocity to hold.

$$\frac{U_g}{\epsilon} - U_p = U_p = \epsilon^n U_T^* \quad (14)$$

The average slip velocity is calculated and compared to the right hand side of Equation 14 in Figure I-5 for three solid rates.

It is clear that throughout the dense conveying regime Equation 14 overestimates the actual (average) slip velocity -

$$U_{\text{slip}} < \epsilon^n U_T^* \quad (15)$$

Moreover, while Equation 14 predicts an increase in the slip velocity as the voidage is increased (because of an increase in the value of ϵ^n , i.e., a decrease in the magnitude of the hindered settling effect) the actual slip velocity peaks at around $\epsilon = 0.97$ and then decreases, approaching U_T as the voidage approaches the value 1.0. It seems then that, as was pointed out before, the

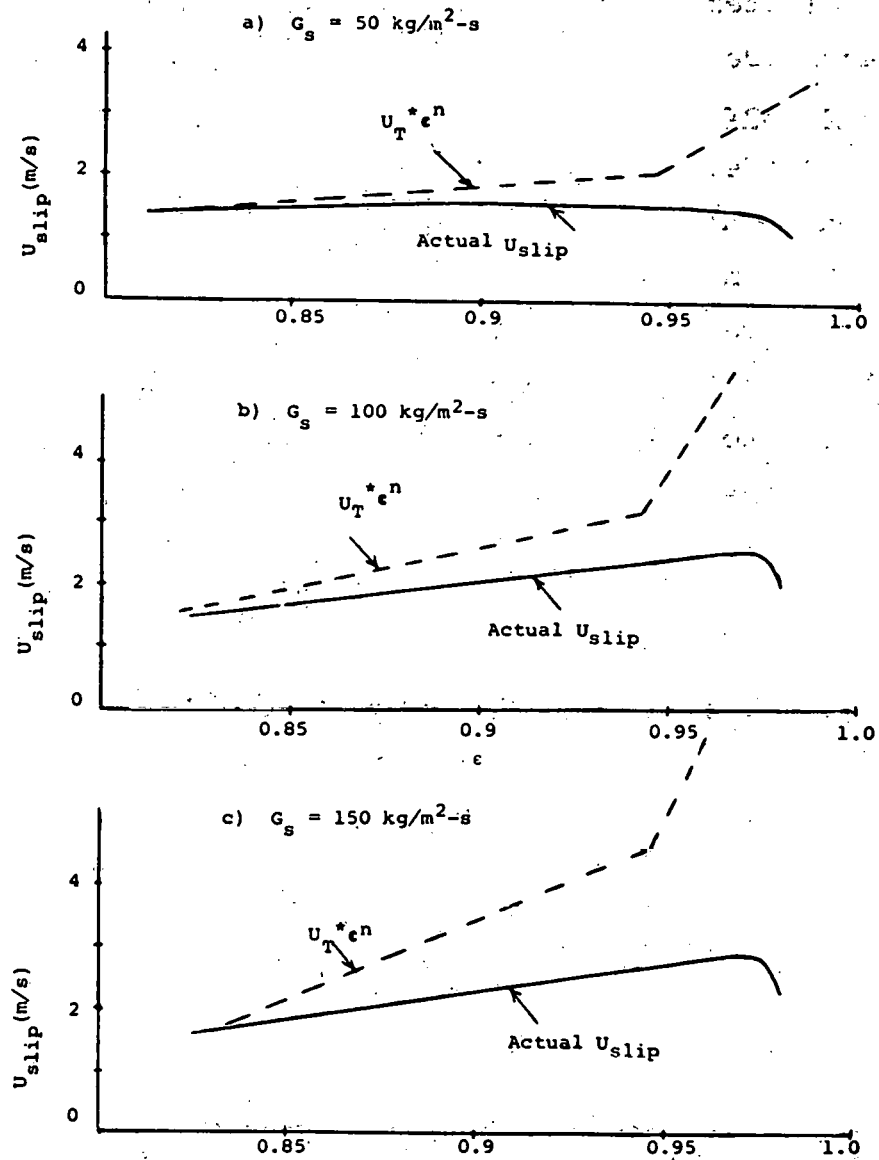


Fig. I-5. The slip velocity in the dense conveying and fast regime.

phenomenon of clustering is much more complex than a single model of rigid spheres would predict. One possible explanation would seem to be as follows: while U_T^* is a measure of cluster size, one has to take the cluster voidage into account as well. It stands to reason that when voidage is increased (by increasing the superficial gas velocity) the clusters have more "room" to move. Two parallel phenomena might be taking place: a) the clusters expand and their voidage ϵ_c is larger than at lower bed voidage values. Thus, more gas passes in the interstitial voidage of the cluster, causing the single particle properties to come more into play. This was alluded to before, in the use of Equation 9. The overall slip velocity then would lie between the high value caused by $\epsilon^{nU_T^*}$ and the much lower value predicted by $\epsilon^{nU_T^*}$. Note also that the two voidages used in these two expressions are not strictly the same. The first implies an apparent porosity, while the latter takes into account a porosity closer to the cluster voidage, ϵ_c . b) The higher gas velocity is exerting a larger shearing stress on the down-flowing phase. Thus, clusters would recirculate less than at lower gas velocities. This phenomenon of decreased down-flow velocity at superficial gas velocities higher than 3 m/s is corroborated later by our solid mixing results.

These two factors, a lower down-flow velocity and a higher cluster voidage offer one possible explanation for the deviation of the actual slip velocity from that predicted by Equation 14.

When one goes into the fast fluidization regime, depicted in Figure I-4.d, the voidage decreases and solid recirculation becomes predominant. The actual slip velocity approaches the theoretical prediction of Equation 14 (Figure I.5) and seems to equal it exactly at the onset of the fast fluidization regime for all solid rates investigated. Note that different values of n and U_T^* are used in the fast fluidization regime. Following the same logic one may

presume that clusters behave more as tightly packed spheres in the denser fast fluidization regime. The denser the suspension - the denser are the clusters and thus their terminal velocity, corrected for the voidage, approximately equals the actual slip velocity. It is interesting to note that Equation 14 seems to be exactly satisfied at U_{TR} , the transport velocity, for all solid rates investigated. This seems to offer another method for calculating U_{TR} , and it agrees well with the picture of this transition as presented in the introduction to this work.

The transport velocity is thought of as the velocity which would cause the entrainment of the largest possible clusters. As the voidage is increased beyond the voidage at U_{TR} the actual slip velocity is less than that predicted by Equation 14 for the same reasons discussed before: the clusters expand, allowing more gas to percolate through them, and less recirculation is taking place at the higher gas velocities.

I.1.4 REFERENCES

- Avidan, A.A. (1979), Flow Patterns in High-Velocity Fluidized Beds, Proposal for Doctoral Research, Department of Chemical Engineering, The City University of New York.
- Capes, C.E. (1974), "Particle Agglomeration and the Value of the Exponent n in the Richardson-Zaki Equation," Powder Tech., 10, 303-306.
- Carotenuto, L., Crescitelli, S. and Donsi, G. (1974), "High Velocity Behavior of Fluidized Beds: Characterization of Flow Regimes," La Chimica e l'Industria (Suppl.), 10, Vol. 12, 185.
- DeLasa, H. and Gau, G. (1973), "Influence des Agregats sur le Rendement d'un Reacteur a Transport Pneumatique," Chem. Eng. Sci., 28, 1875-1884.
- Massimilla, L. (1971), "Behavior of Catalytic Beds of Fine Particles at High Gas Velocities," AIChE Symposium Series, 128, Vol. 69, 11-13.

REFERENCES (cont.)

- Mogan, J.P., Taylor, R.W. and Booth, F.L. (1969), "A Method of Prediction of the Porosities of High-Pressure Gaseous Fluidization Systems," The Can. J. of Chem. Eng., 47, 126-130.
- Mogan, J.P., Taylor, R.W. and Booth, F.L. (1970/71), "The Value of the Exponent n in the Richardson-Zaki Equation for Fine Solids Fluidized with Gases Under Pressure," Powder Tech., 4, 286-289.
- Richardson, J.F. and Zaki, W.N. (1954), "Sedimentation and Fluidization: Part I," Trans. Instn. Chem. Engrs., 32, 35-53.
- Rowe, P.N., Santoro, L. and Yates, J.G. (1978), "The Division of Gas Between Bubble and Interstitial Phases in Fluidized Beds of Fine Powders," Chem. Eng. Sci., 33, 133-140.
- Yerushalmi, J., Cankurt, N.T., Geldart, D. and Liss, B. (1978), "Flow Regimes in Vertical Gas-Solid Contact Systems," AIChE Symp. Ser. No. 176, Vol. 74, 1-13.

I.2 WORK FORECAST FOR THE NEXT QUARTER

Work in the next quarter will concentrate on solid mixing experimentation in the expanded top bed. Preliminary work in this area was described in the ninth and tenth quarterly reports. An experimental setup consisting of a 15.2 cm I.D. expanded top bed was constructed and a ferromagnetic tracer system was installed in it. This system will be improved upon and results in the low velocity fluidization regimes (bubbling and slugging) will be sought with HFZ-20. We will also try to get some data in the turbulent fluidization regime.

II. FLASH HYDROGENATION

II.1 WORK ACCOMPLISHED

II.1.1 Yield Correlations

We have previously (see 11th Quarterly Report) explored the relationship between total hydrolysis yield and coal rank, petrographic composition, and aliphatic hydrogen and oxygen content. Here we develop correlations for the various products separately.

For purposes of empirical prediction, correlations in two variables have been formulated using the technique of stepwise regression (1). The field of independent variables used to describe the coals include: the petrographic composition, the elemental composition, and the mineral matter, volatile matter and the reactive maceral (the sum of vitrinite, pseudo-vitrinite, exinite and resinite) contents all on a dmmf basis. These variables amount to a total of 16. The dependent variables of interest are: the total conversion to volatiles and the yields of methane, ethane, CO_x, BTX and total liquids. In all cases the dependent variables are from experiments performed at 300°C, 10 seconds contact time and 0.6 seconds vapor phase residence time. Yields are expressed as percentage of the initial carbon converted to the product considered.

A stepwise regression was carried out with each dependent variable as a linear function of the independent variables. In all cases, two variables were necessary to yield correlations whose standard deviation was of the order of magnitude expected from the accuracy of the experimental data. The resulting relations, from all possible variable pairs, were compared according to their correlation coefficient (ρ) and standard deviation (σ) and the best fit chosen. The parameters obtained in the correlations are valid to predict yields under the reaction conditions employed in these experiments. The parameters are expected to change with the reaction conditions.

The best correlation for the total conversion of coal to volatiles was obtained with exinite content and mineral matter as independent variables. It shows a correlation coefficient close to one, and a standard deviation close to the standard deviation of the experimental data (See Figure II-1). The content of mineral matter appears in the correlation with a negative coefficient, indicating that increased mineral matter will decrease the yield of total volatiles in flash hydrogenation. Although for the short residence times and high temperatures used in flash hydrogenation experiments, the catalytic effect of the mineral matter should be minimal (in contrast with the results obtained in coal liquefaction, at low temperatures and longer residence times), the presence of a negative effect is quite unexpected.

The strong correlation of total yield of volatiles with exinite content indicates that this is the most important variable in the correlation. A discussion of this point was given in the last quarterly report.

The technique of stepwise regression is also applied to the individual species. The correlations for the yields of methane, ethane, BTX, carbon oxides and heavy liquids are presented in Table I-1 and Figures II-2 to 6.

The best correlation for methane yields are with pseudo-vitrinite and sulphur. Sulphur, in the correlation, appears with a negative coefficient. This fact contrasts with the results from coal liquefaction (2) where a positive effect of sulphur content is observed.

Ethane yields correlate with vitrinite and sulphur content. Again, sulphur appears with a negative coefficient in the correlation.

BTX yields correlate with vitrinite and fusinite content. The coefficients for both macerals are negative.

The yields of carbon oxides correlates with the oxygen and hydrogen contents. In this case, the observed positive correlation with oxygen is to be expected, since in flash hydrogenation the only

Table II-1

SUMMARY OF CORRELATIONS OF YIELDS WITH COAL PROPERTIES

Fixed reaction conditions: 800°C, 100 atm H₂, 10 seconds solid contact time.
0.6 seconds gas residence time.

TOTAL VOLATILES = 54.54 + 3.93 (Exinite) - 0.49 (Mineral Matter)

$$\rho = 0.94 \quad \sigma = 2.4 \%$$

METHANE = 17.97 - 0.5 (Sulphur) + 0.33 (Pseudo-Vitrinite)

$$\rho = 0.97 \quad \sigma = 0.87 \%$$

TOTAL LIQUIDS = 2.55 (Carbon) - 4.2 (Sulphur)

$$\rho = 0.96 \quad \sigma = 2.92 \%$$

CARBON OXIDES = 26.63 + 0.35 (Oxygen) - 4.3 (Hydrogen)

$$\rho = 0.99 \quad \sigma = 0.62\%$$

BTX = 16.65 - 0.08 (Vitrinite) - 0.58 (Fusinite)

$$\rho = 0.88 \quad \sigma = 0.87 \%$$

ETHANE = 1.44 + 0.086 (Vitrinite) -) .35 (Sulphur

$$\rho = 0.98 \quad \sigma = 0.19 \%$$

HEAVY LIQUIDS = 5.29 + 5.64 (Exinite) - 0.71 (Pseudo-Vitrinite)

$$\rho = 0.97 \quad \sigma = 2.4 \%$$

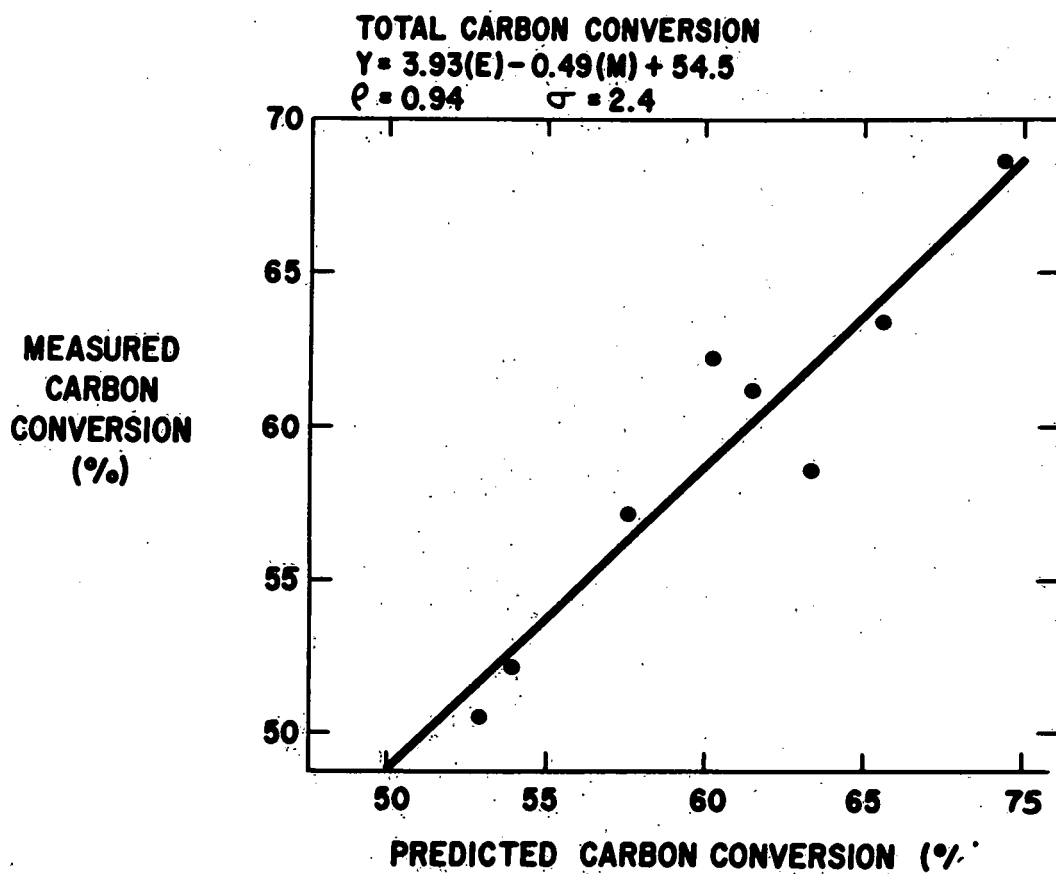


Figure II-1. Correlation for Total Carbon Conversion

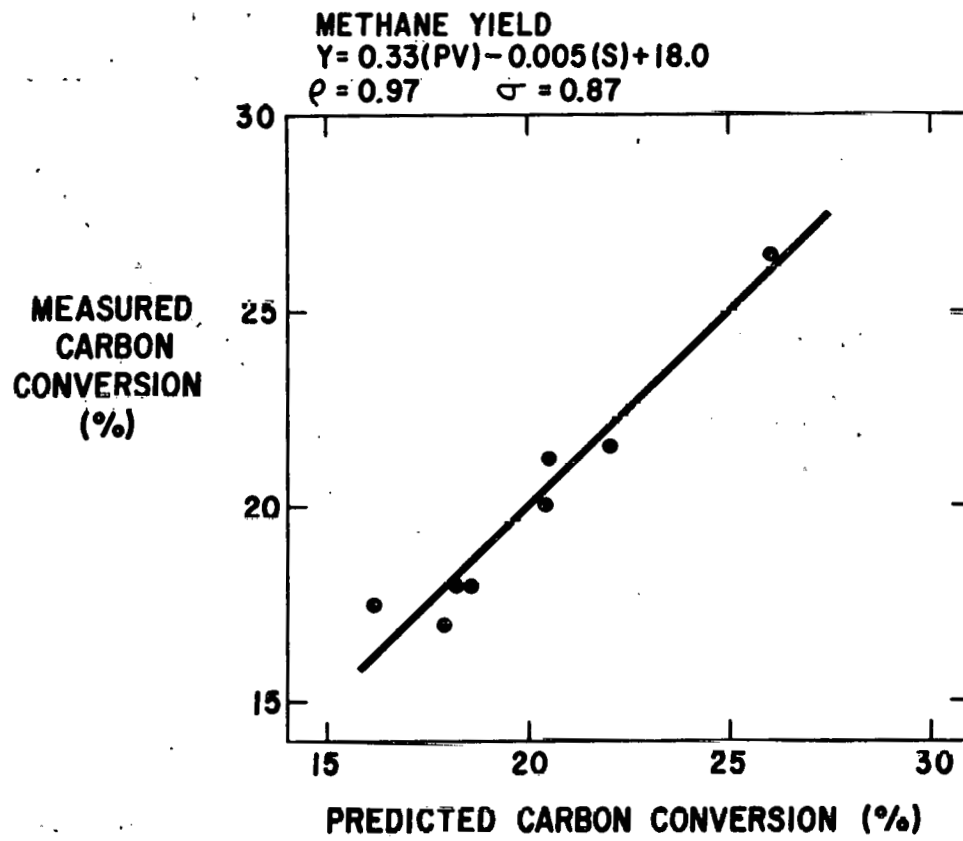


Figure II-2. Correlation for Methane Yield

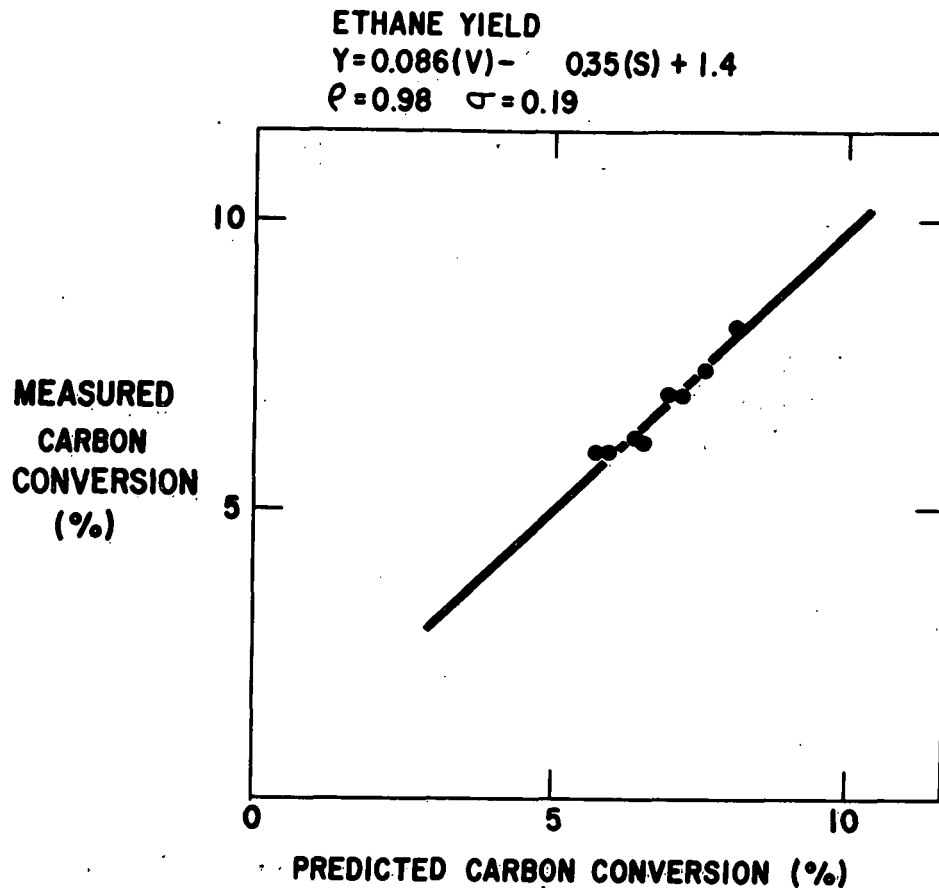


Figure II-3. Correlation for Ethane Yield

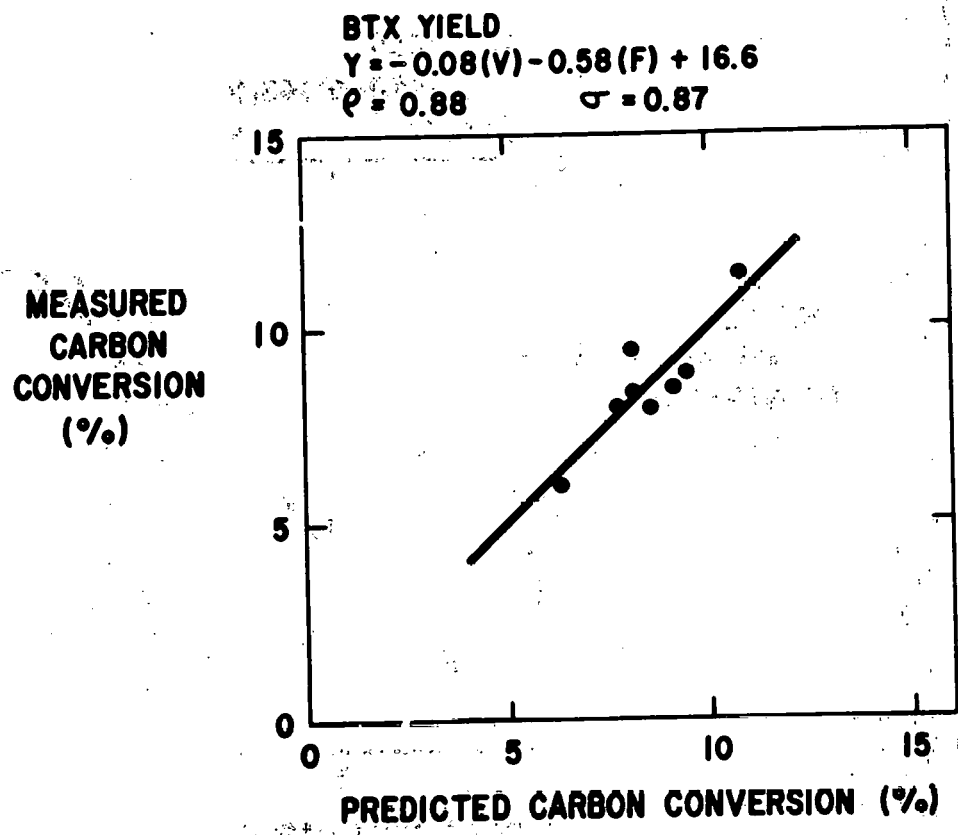


Figure II-4. Correlation for BTX Yield

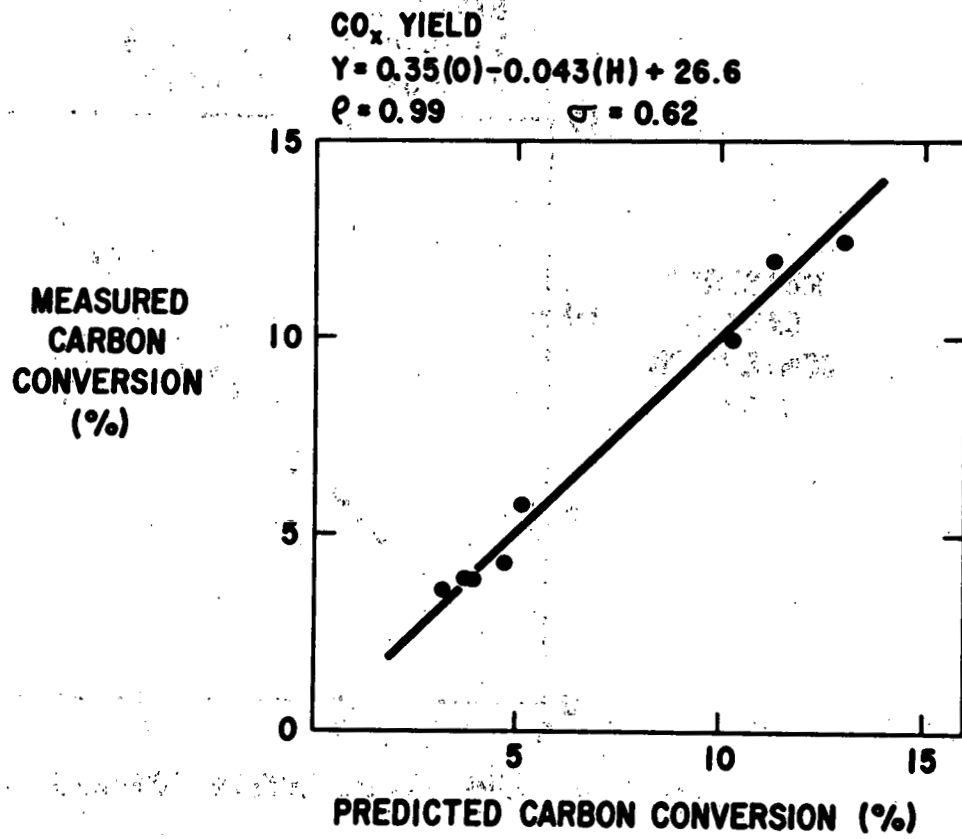


Figure II-5. Correlation for Total Yield of Carbon Oxides

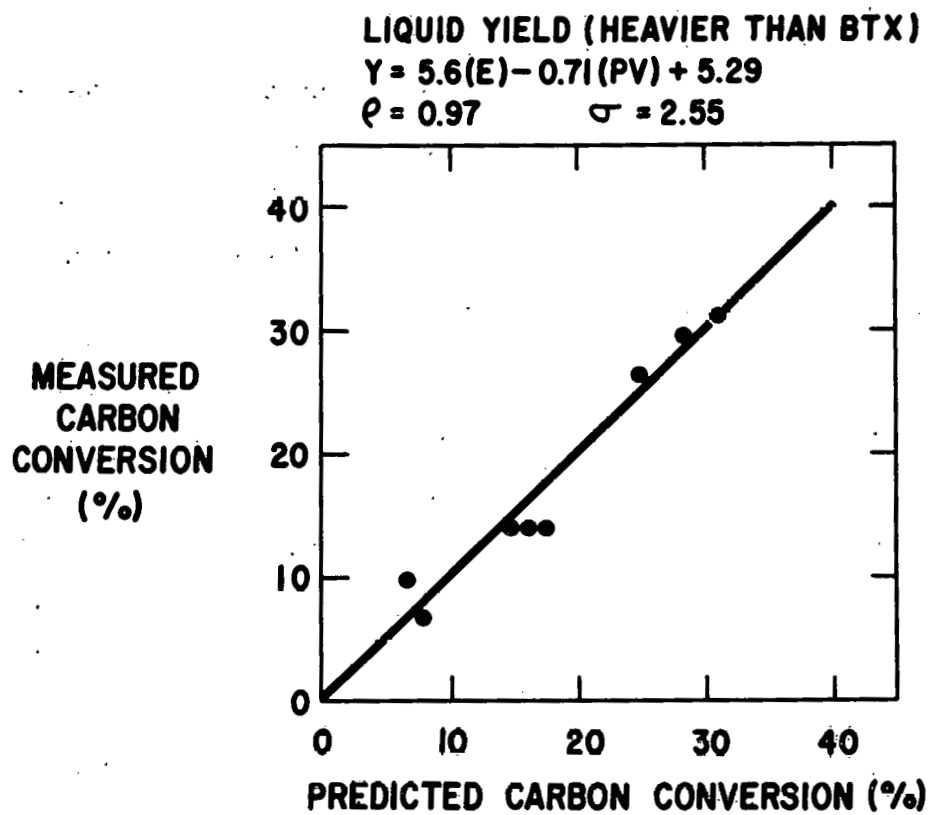


Figure II-6. Correlation for Yield of Liquids Heavier than BTX

source of oxygen is what is contained in the coal. Hydrogen content appears to decrease the yields of carbon oxides.

The yields of liquids heavier than BTX correlates with exinite and pseudo-vitrinite. Again, exinite appears with a coefficient larger than one, indicating that it promotes the production of liquids.

All correlation coefficients are about 0.9 or better, and the standard deviations are all quite low. The largest ones, $\sigma = 2.55\%$ for heavy liquids and $.24\%$ for total volatiles, are about the same as the standard deviation obtained from the experimental scattering of the data for these two yields.

II.1.2 Discussion

The reactions involved in coal flash hydrogenation can be visualized as occurring in two stages. In a first stage, in a solid or plastic phase coal decomposes thermally as in pyrolysis, yielding light gases and large fragments that are a part of the original coal structure. In the second stage, occurring in the gas phase, the fragments undergo hydrogenation and further hydrocracking to yield light gases and light aromatic species. With this description of the sequence of events, it follows that flash hydrogenation may be modelled with the combination of a coal pyrolysis (or hydro-pyrolysis model) model, and a model of the thermal hydrocracking reactions in the vapor phase.

A model of coal pyrolysis, based on free-radical kinetics and a set of "structural parameters" for the coal, has been proposed by Gavalas and co-workers (3). In this model, the structure of the coal affects the initial conditions used to start the integration of a set of non-linear differential equations that describes the behavior of the chemical reactions involved in the model. The kinetic constants are assumed to be "universal", or to depend weakly on coal properties (4).

A more simplified model of coal pyrolysis was proposed by Solomon and Colket (4). This model is based upon first order kinetics. It also contains a set of "structural parameters" which are visualized as the initial content of functional groups in the coal. These groups can be measured by different analytical techniques. Solomon's structural parameters are used as initial conditions in the integration of the differential equations describing his kinetic model, which also contains "universal" kinetic constants.

In both models coal properties enter through the "structural parameters" of the coal, which are the initial conditions of the model differential equations. In both cases, it is possible to assume a linear relationship between the specified structure parameters and the properties of the coal, as measured by more conventional techniques.

With respect to the reactions in the gas phase, the simultaneous thermal decomposition and hydrogenation of hydrocarbons has been modeled using free-radical kinetics (5) and also using more simplified approach, in the case of constant hydrogen pressure (6). The simplified approach leads to a system of first order reactions.

It is possible to build a flash hydrogenation model with a simplified pyrolysis model, such as the one proposed by Solomon and Colket, and a simplified gas phase reaction model. In this case both chemical processes are modeled with first order chemical reactions and with "universal" kinetic constants. Thus, the model of coal flash hydrogenation will contain the properties of the coal in the initial conditions of a set of differential equations representing the behavior of the coal. Consequently, using the general theory of first order kinetic network (7) and under fixed reaction conditions, the yield of each of the individual species is a linear combination of the initial conditions, or more precisely, is a linear

combination of the coal properties. This important conclusion gives a theoretical basis to the empirical correlations given here.

An extension of the correlations given here, integrating coal properties and process conditions in flash hydrogenation, is most desirable. Such a model would be very useful in predicting yields for various coals and different operating conditions, knowing only the properties of the coals.

II.1.3 Liquids Characterization

Elimination of interference of silica gel in SESC fractions

After washing the silica gel used in the SESC separation with methanol and with acidified distilled water, it was found that the SESC fractions still contained considerable amounts of silica gel particles. As a result, the gravimetric determination of the fractions still would be inaccurate due to the presence of this material. Alternative methods of quantifying the amount of samples have to be considered.

Pressure gel permeation chromatography

The GPC technique in use has the inconvenience of being time-consuming. (Taking about 2 to 4 hours per analysis). In order to reduce the time of analysis, an Altex μ -Spherogel 100Å steric exclusion chromatography column has been put into use. Analysis with the new column takes about 15 minutes. Figure II-7 shows the calibration curve, using polystyrene standards of known molecular weight.

Figure II-8 shows the normalized traces from the GPC of flash hydrogenation liquids, other coal-derived liquids and tar sands. The analysis is very useful for comparison purposes although the molecular weight scale corresponds to the standards used and the U.V. detector response was not corrected.

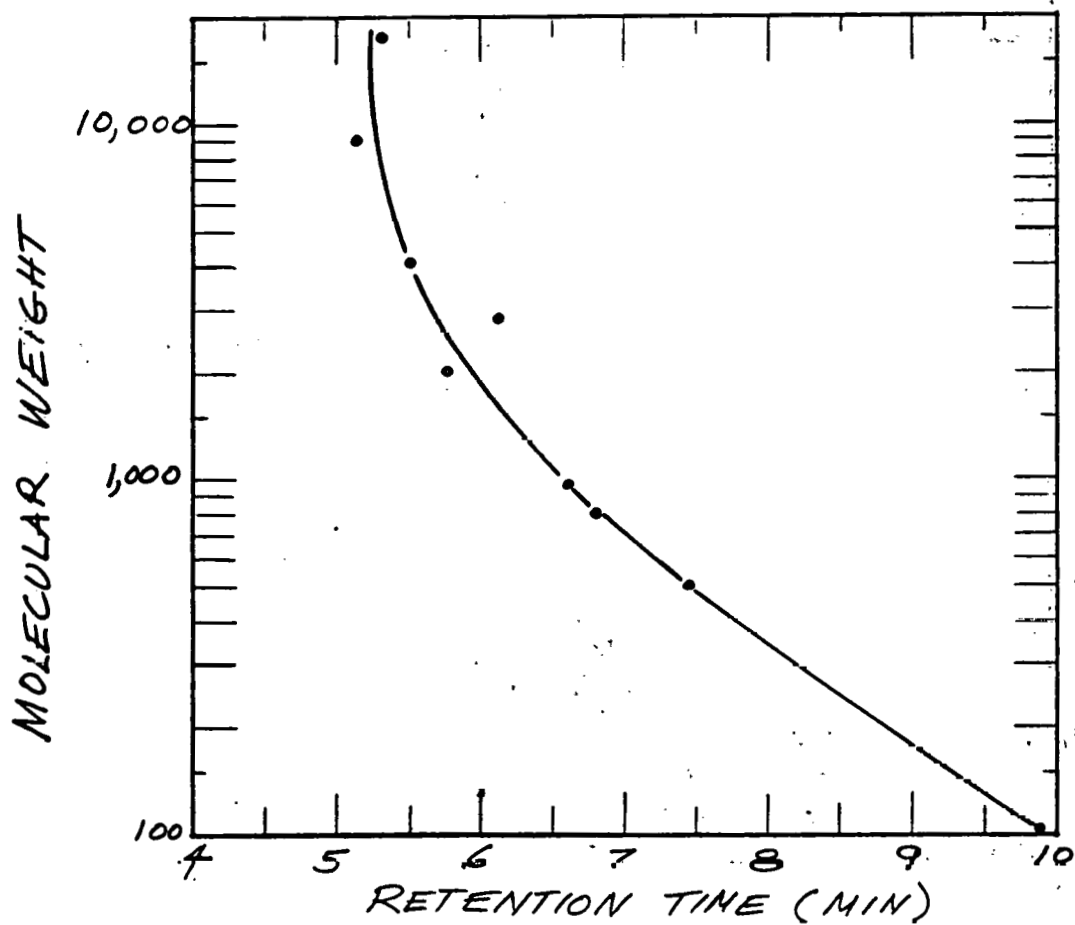


Figure II-7. Calibration of Steric Exclusion Chromatography Column (100 A μ -Spherogel) with Polystyrene Standards

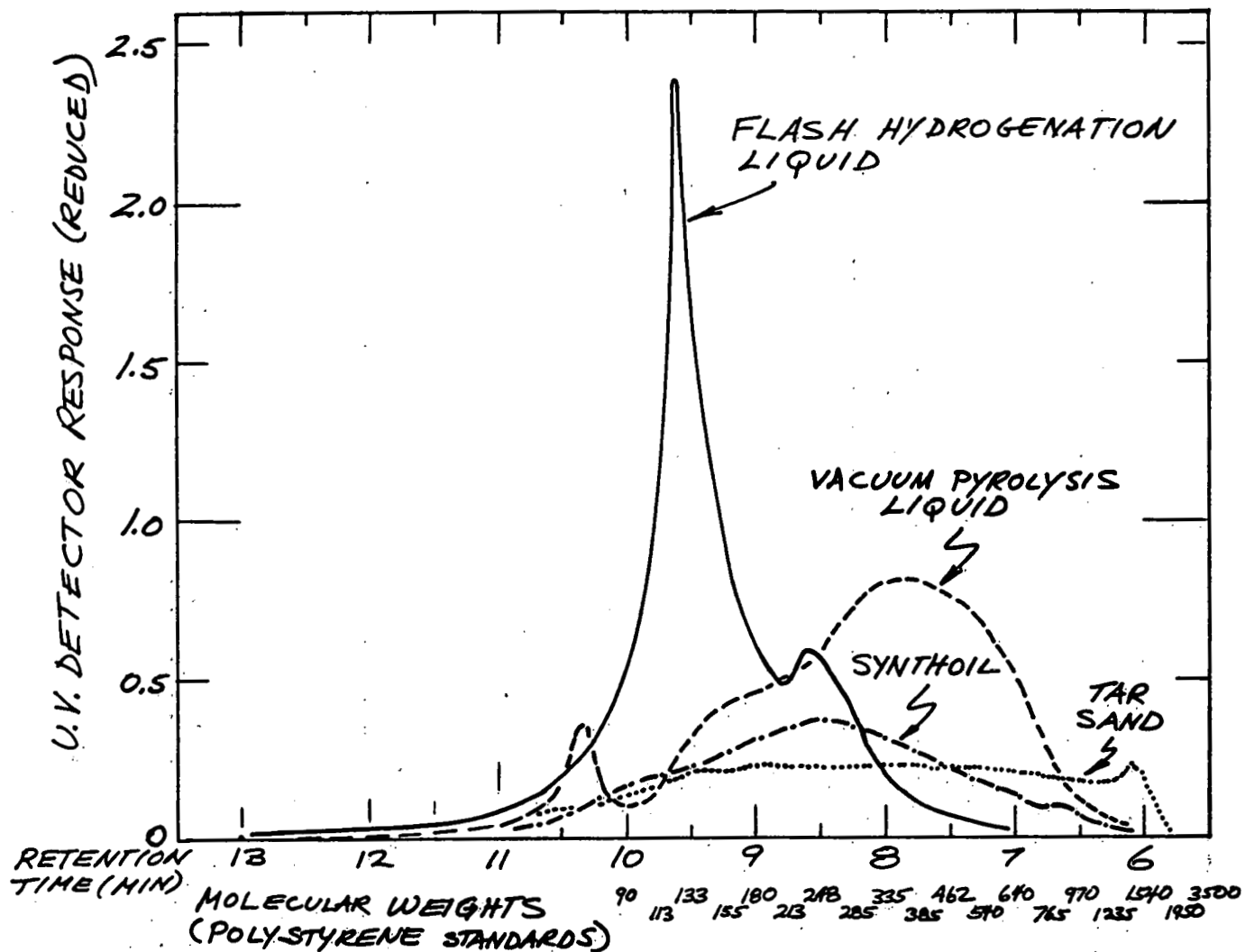


Figure II-8. Molecular Weight Distribution of Illustrative Synthetic Liquids.

Flash Hydrogenation Liquid: from PSOC 170 coal at 715°C, 0.6 sec. v.r.t., 100 atm. H₂, The City College.

Vacuum Pyrolysis Liquid: from PSOC 170 coal at 465°C, P. Solomon, United Technologies Research Center.

Synthoil: U.S. Bureau of Mines.

Tar Sand: Athabasca ARII, W. Seitzer, Sunoco.

II.2 WORK FORECAST FOR THE NEXT QUARTER

A study of two-stage flash hydrogenation will be initiated in the next quarter. Separate control of devolatilization temperature and hydrocracking temperature adds a degree of freedom in process optimization.

A carbon content analyzer is being constructed to analyze the samples from the SESC separation. It is expected that this unit will start yielding results in the next quarter. This will allow the use of SESC and GPC in the characterization of liquids from flash hydrogenation runs.

III. FLASH HYDROLYSIS

III.1 WORK ACCOMPLISHED

In order to study the effect of heating rate on flash hydrolysis yield, a modification of the electrical system is required. The modification, made during this quarter, consists of interposing a pair of variable transformers between the system and the line

As a result of voltage losses in these transformers the maximum heating rate is limited to 250°C per second. In addition, each setting of the line voltage transformers requires a readjustment of variable transformer 6 which controls reactor power during the constant temperature period. An extensive set of calibrations is consequently required to establish the settings on both sets of transformers for a desired heating rate and a desired final temperature, each of which can be independently controlled.

The modification has been installed and tested. Calibration for a reaction temperature of 800°C have been established.

III.2 WORK FORECAST FOR NEXT QUARTER

During the next quarter a series of runs will be conducted establishing the effect of heating rate on flash hydrolysis yield.

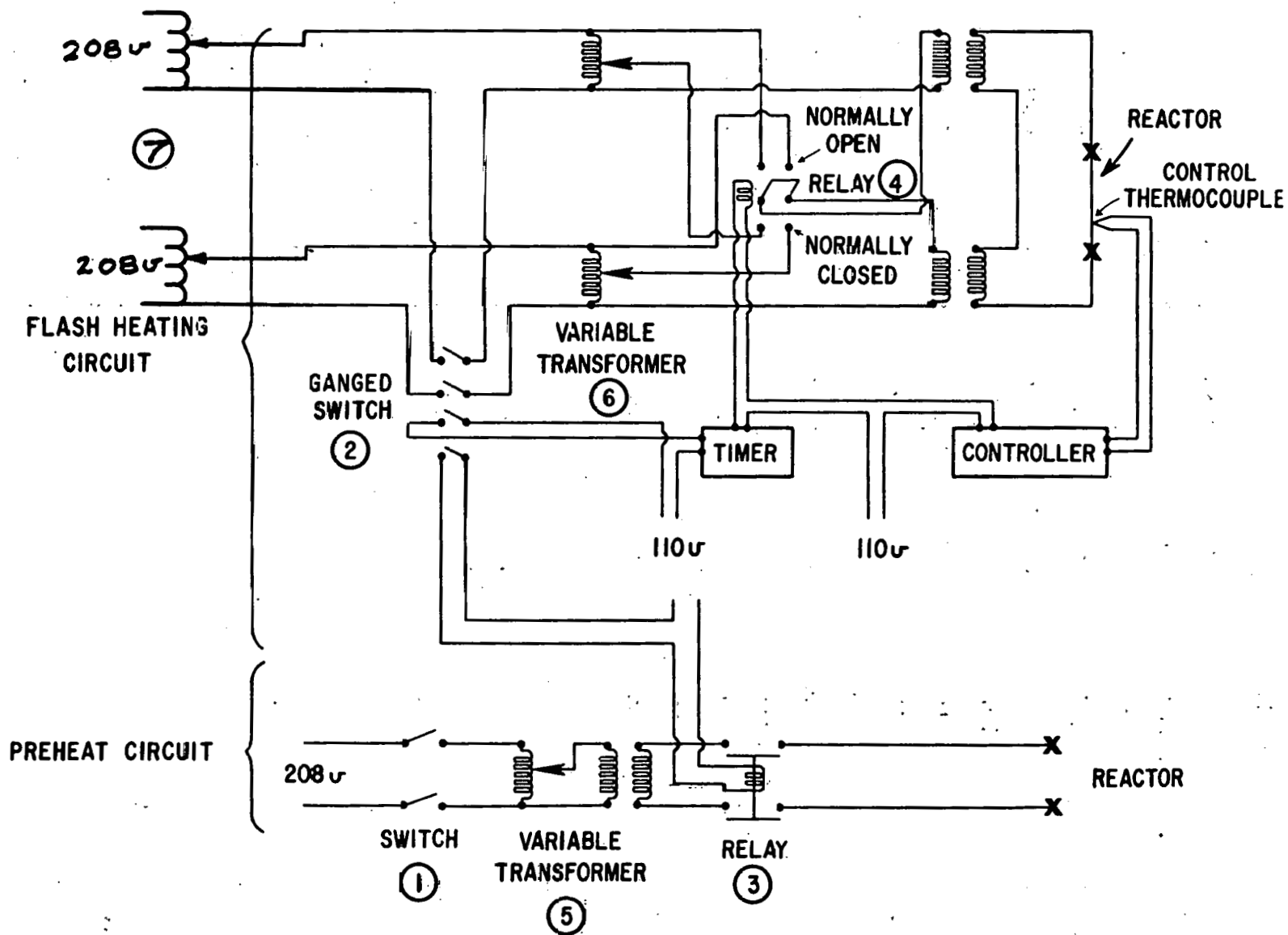


Figure III-1. Electrical Schematic of Flash Hydrolysis System Modified for Variable Heating Rate by the Addition of Adjustable Transformers 7.

CONCLUSIONSI. HIGH VELOCITY FLUIDIZED BEDS

1. Bed expansion of all group A powders investigated can be described by a modified Richardson-Zaki correlation, $U_g/U_T^* = \epsilon^n$. While U_T^* and n vary predictably with particle properties for known size distribution; it is the latter parameter that is of utmost importance. Changes in size distribution will have a profound effect on bed expansion properties.

2. All three group A powders used in this investigation can be described by the same expansion equation in the "dense conveying" regime ($0.945 < \epsilon < 0.98$). It is possible that because of the high voidages, all group A powders show the same expansion behavior in this regime, regardless of particle properties.

3. The index n in the modified Richardson-Zaki approach is thought of as a measure of the homogeneity of a fluidized bed. It is high in the aggregative, slugging regime, and it drops to its normal value for fine powders, in the turbulent regime ($n = 10$ in the slugging regime, $n = 5$ in the turbulent regime).

4. High values of the exponent n were thought of as anomalous in the reported literature for fine powders, and Capes (1974) presented a method to explain them by considering particle aggregation. A similar approach by Yerushalmi is shown to give estimates of cluster voidage. The cluster voidage in the turbulent regime is shown to be close to minimum fluidization voidage. In the fast bed the cluster voidage depends on solid rate and does not change much with gas velocity. "Equivalent" cluster diameters are also calculated from the exponent n and they show an order of magnitude agreement to cluster diameter calculated by other methods.

5. While the index n is not a function of size distribution, U_T^* (thought to represent the effective cluster terminal velocity) is. This effective cluster velocity, calculated from the experimental

results, is shown to throw some light on the phenomenon of clustering. Clustering is shown to be a complex dynamic phenomenon. Particles move in and out of clusters rapidly and thus clusters cannot be thought of as "hard spheres" of the equivalent cluster diameter, except at the lower end of the fast fluidization regime. At the latter point the average slip velocity is shown to equal $\epsilon^n U_T^*$, thus supporting the "hard sphere" model. As the gas velocity is raised, the clusters are thought to have a higher degree of freedom and the single particle properties come into play as well, causing the average slip velocity to be lower than $\epsilon^n U_T^*$. The slip velocity peaks in the dense conveying regime and is thought to approach the single particle terminal velocity as the voidage approaches unity.

A uniform suspension does not seem to form with fine powders even at very high voidages, and so instead of $U_{\text{slip}} < U_T$ (hindered settling), one always observes $U_{\text{slip}} \gg U_T$. In other words, while U_T serves as the lower limit to the slip velocity in the fast and dense conveying regimes, $\epsilon^n U_T^*$ is the higher limit. This is thought of as representative of the dual nature of clusters: as "hard spheres" (ϵU_T^*) and as single particles (U_T).

II. FLASH HYDROGENATION

1. Yields from U.S. coals ranging from lignite through bituminous are correlated to within experimental accuracy by linear relations in two independent variables. These correlations are listed in Table II-1.

2. Exinite is a promoter for the formation of heavy liquids from other macerals.

3. Flash hydrogenation liquids are predominantly in the 90 to 400 molecular weight range.

III. FLASH HYDROLYSIS

None this quarter.